Available online at www.sciencedirect.com

ScienceDirect

Procedia CIRP 74 (2018) 300–304

www.elsevier.com/locate/procedia

10th CIRP Conference on Photonic Technologies [LANE 2018]

Influence of laser spot size and shape on ablation efficiency using ultrashort pulse laser system

Michalina Chaja[a,]*, Thorsten Kramer[a], Beat Neuenschwander[a]

[a]*Bern University of Applied Sciences, Institute for Applied Laser, Photonics and Surface Technologies, Pestalozzistrasse 20, CH-3400 Burgdorf, Switzerland*

* Corresponding author. Tel.: +41 34 426 43 54 ; fax: +41 34 426 43 54. *E-mail address:* michalinaweronika.chaja@bfh.ch

Abstract

Ultra-short pulsed laser systems provide high accuracy and high-quality materials processing for various kinds of applications. However, one of the highest industrial needs is to identify most efficient processes to achieve high throughput. In terms of ultra-short pulsed laser processing of metals, the specific removal rate (ablated volume per time and average power) shows a maximum value i.e. there exists an optimum fluence where the ablation process is most efficient. In this study the influence of spot size and shape (Gaussian and Top Hat) on the ablation efficiency on AISI 304 (1.4301) steel grade was examined using 10 ps and 350 fs laser pulses at wavelengths of 1064 nm and 1030 nm. The investigation revealed a significant drop of the specific removal rate with increasing Gaussian spot size for both pulse duration. While this behaviour is less pronounced for a Top Hat, showing just 8% decrease of specific removal rate for spot sizes bigger than 40 µm.

Peer-review under responsibility of the Bayerisches Laserzentrum GmbH.

Keywords: ultrashort laser pulses; laser spot size; specific removal rate; ablation efficiency; Top Hat

1. Introduction

The great benefits referred to ultrafast laser systems as high accuracy and high quality of ablated structures have been revealed in many studies [1,2]. However, the still recurring problem of the industry sector is to identify the most efficient process to achieve highest throughput [3,4]. In case of ultrafast laser micro processing, the throughput can be described by the specific removal rate, meaning the ablated volume per time and average power, i.e. the ablated volume per pulse energy [4,5]. It was already shown that the specific removal rate can be optimized by working at optimum fluence. Other processing parameters like pulse duration, repetition rate, pulse bursts or scanning strategy can significantly influence the efficiency of the ablation process [3-9]. The influence of the spot size for the first time was reported in the late 80s showing an increase of the ablation rate by a factor of 3 when compared with larger spot size [10]. These findings were followed by similar results for different laser pulse durations (ns, ps, fs) and wavelengths (UV, VIS, IR) for wide range of materials [10-16]. In the literature exist some possible explanations for this behavior, like increased plume shielding at larger spots or influence of the crater aspect ratio on the hydrodynamics of post-pulse ablation [10-13].

Despite the broadly discussed topic of spot size on laser ablation efficiency, the influence of the different laser beam shape and its size change was so far omitted. In this study, as an extension for gaussian spot size (in ps and fs range) influence on specific removal rate, the Top Hat beam shape size was investigated. Craters were machined with different fluences (considering the geometrical differences of Gaussian and Top Hat profile) to obtain the maximum specific rate.

2. Experimental setup

The experiments were carried out by using a FUEGO^{TM} from LUMENTUM (former Time Bandwidth Products, Switzerland) a 10 ps laser system working at a wavelength of 1064 nm and a Satsuma HP2 laser system from Amplitude Systèmes, working at 1030 nm wavelength with pulse

Peer-review under responsibility of the Bayerisches Laserzentrum GmbH.
10.1016/j.procir.2018.08.119

duration of 350 fs. Both systems ran at their full power and the average power was adjusted by utilizing an external attenuator, consisting of a λ/2 waveplate and a thin film polarizer. After passing through the attenuator the beam was guided via a λ/4 waveplate (for generating circular polarization) with folding mirrors through a beam expander into different focusing components. To achieve a Top Hat beam shape, Top Hat Beam Shaper FBS2 from TOPAG was placed in front of the beam expander and adjusted to 0^{th} order using a 1000 mm focal lens and beam profiling camera. Spot sizes and M^2 were measured with a scanning slit beam profiler (BP209) from Thorlabs. The focal plane was always set to the sample surface. The experiments were performed on stainless steel 1.4301 (AISI 304). The sample surface was polished with a 3 µm diamond suspension. After the ablation process, the samples were cleaned in an ultrasonic bath with isopropanol. The structures were analyzed by using a whitelight interference microscope (SmartWLI) from GBS.

2.1. 10 ps pulse duration

Different optical components were used to obtain 10 different Gaussian spot sizes (w_0) and 6 different square alike Top Hat spot sizes (a). Beam quality factor (M^2) was below 1.3. To exclude heat accumulation effects, the repetition rate was reduced to 50 Hz with pulse on demand (POD) option. To calculate the specific removal rate, the craters were machined with different laser peak fluences for 100 and 250 pulses per crater. To guarantee statistical significance 5 craters per fluence per number of pulse were ablated. With measured crater volume for both beam profiles, the specific removal rate can be calculated according to [14]:

$$\left(\frac{V}{P_{av}}\right)_{crater} = \frac{\Delta V}{{}^{n}\!/_{f_{rep}} \cdot \left(E_p \cdot f_{rep}\right)} = \frac{\Delta V}{n \cdot E_p} = \frac{\Delta V \cdot f_{rep}}{n \cdot P_{av}} \quad (1)$$

In which n denotes number of pulses, P_{av} the used average power and f_{rep} the laser repetition rate. To determinate the two material parameters threshold fluence ϕ_{th} and energy penetration depth δ, influencing specific removal rate, the well-known logarithmic ablation law was used [1]:

$$z_{abl} = \delta \cdot \ln\left(\frac{\phi_0}{\phi_{th}}\right) \quad (2)$$

Where ϕ_0 indicates peak fluence calculated respectively for Gaussian and Top Hat profile accordingly to [4,17]. Measuring the depth of the crater and using the logarithmic ablation law (2), the threshold fluence ϕ_{th} and the energy penetration depth δ can be deduced from the experimentally obtained data. With these values, the theoretical maximum specific removal rate can be calculated by using [18]:

$$\left(\frac{V}{P_{av}}\right)_{\max\ GAUSS} = \frac{2}{e^2} \cdot \frac{\delta}{\phi_{th}} \quad (3)$$

$$\left(\frac{V}{P_{av}}\right)_{\max\ TOP\ HAT} = \frac{1}{e} \cdot \frac{\delta}{\phi_{th}} \quad (4)$$

One of the possible ways to compare the Gaussian beam profile and the Top Hat shape is by using the beam area, however possible beam extension in one direction (ellipsis) could strong influence the Gaussian beam area. Thus, the average diameter ($2w_0$) for Gauss spot and diagonal ($a\sqrt{2}$) for Top Hat square was used

2.2. 350 fs pulse duration

For experiments with Satsuma (350 fs) the galvanometer scanner Intelli*SCAN*de14 from SCANLAB combined with 100 mm or 160 mm f-theta (telecentric) objective was used. Different beam expanders allowed to achieve 6 different spot sizes with M^2 in range of 1.2-1.5.

To determine the specific removal rate, squares were machined with different laser peak fluences for a constant number of machined layers, which amounts to 100. Afterwards from the average of measured depth of the squares d, the specific removal rate can be calculated as follows:

$$\left(\frac{V}{P_{av}}\right) = \frac{\Delta V}{E_p} = \frac{d \cdot p^2}{N_{sl}} \cdot \frac{f_{rep}}{P_{av}} \quad (5)$$

Where p indicates the used pulse to pulse distance (pitch) in x and y direction and N_{sl} the number of machined slices. The repetition rate was set to 505 kHz, while using femtosecond pulse duration contribute to prevent heat accumulation at high repetition rates [19]. The pitch value was calculated to obtain 75% overlap for every spot size. To deduce the threshold fluence and energy penetration depth, the ablation model was used [4,5]:

$$\frac{V}{P_{av}} = \frac{1}{2} \cdot \frac{\delta}{\phi_0} \cdot \ln^2\left(\frac{\phi_0}{\phi_{th}}\right) \quad (6)$$

3. Experimental results

3.1. 10 ps pulse duration

Figure 1 and 2 show the measured specific removal rates for different spot sizes for Gaussian and Top Hat beam shape for 10 ps pulse duration and 250 pulses. Even 20% decrease of specific removal rate for gaussian profile is observed, if radius is increased from 13.4 µm to 68.9 µm, this behavior is less pronounced for a Top Hat, showing just 8% increase of specific removal rate for spot sizes bigger than 40 µm. The optimum peak fluence, where the specific removal rate shows its maximum value, shifts to higher fluences with the increase of the spot size for Gaussian beam profile.

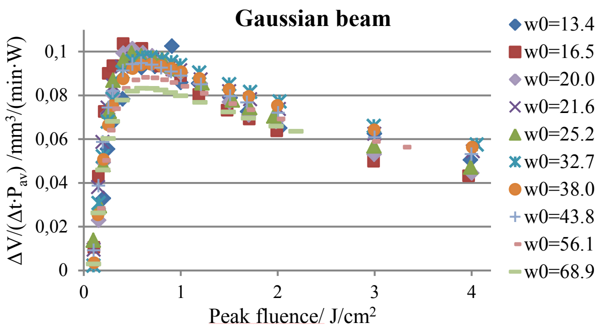

Fig. 1. Influence of the Gaussian beam spot size on the specific removal rate as function of peak fluence for 10ps pulse duration by machining craters.

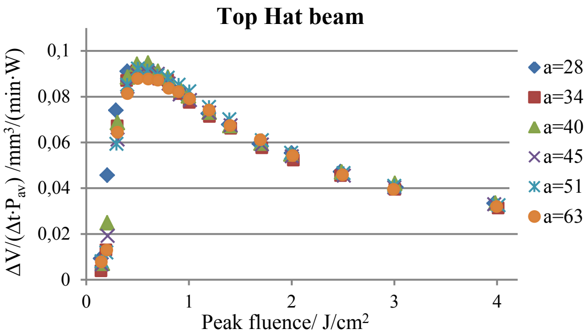

Fig. 2. Influence of the Top Hat beam spot size on the specific removal rate as function of peak fluence for 10ps pulse duration by machining craters.

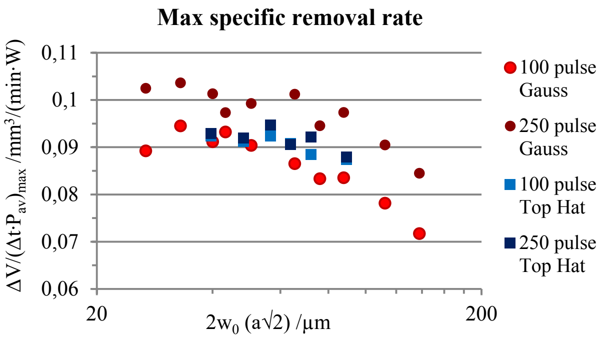

Fig. 3. Influence of the Gaussian and Top Hat beam spot size on the max specific removal rate for 10 ps pulse duration by machining craters.

In figure 3 the maximum specific removal rate as a function of the diameter for a Gaussian and the diagonal for a Top Hat beam profile is presented. Almost a linear drop of the maximum specific removal rate on the Gaussian beam radii greater than 30 µm is visible for both number of pulses. The influence of the applied number of pulses onto the threshold fluence (incubation effect), and thereby also onto the specific removal rate, is still visible for 250 pulses. For a Gaussian beam profile this behaviour causes higher removal rates for 250 pulses compared to 100 pulses whereas for a Top Hat this incubation effect is not observed and the influence onto maximum specific rate is less pronounced. Further investigations of bigger than 60 µm Top Hat sizes (a) are needed to confirm this effect.

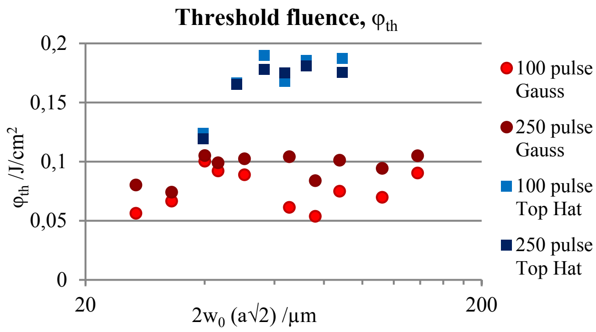

Fig. 4. Influence of the Gaussian and Top Hat beam spot size on the threshold fluence for 10 ps pulse duration by machining craters.

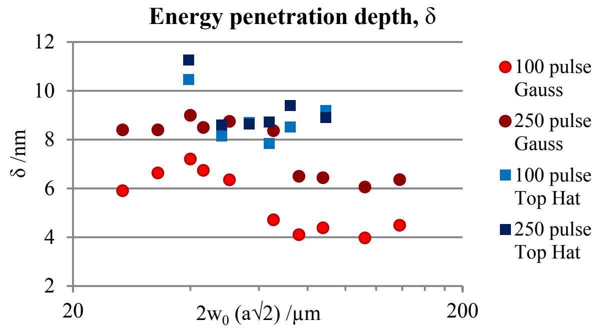

Fig. 5. Influence of the Gaussian and Top Hat beam spot size on the energy penetration depth for 10 ps pulse duration by machining craters.

The theoretical maximum specific removal calculated from (3) and (4) show higher values than the experimentally obtained values. This was also recorded in [20] and explained by measurement of too small volume in case of craters. However, the theoretical values show the same tendency – a decrease of the maximum specific removal rate with increasing spot size.

By plotting the crater depth as a function of fluence and applying the logarithmic ablation law with least square fit, threshold fluence and energy penetration depth were deduced and presented in figure 4 and 5 respectively. For a Gaussian profile, the threshold fluences was varied between 0.10 and 0.05 J/cm^2, which is in a similar range as obtained by Liu method calculated from crater diameter in [4]. For 250 pulses and for radii bigger than 20 µm, the threshold fluence stays at a constant value of approximately 0.1 J/cm^2, and just for the two the smallest radii it drops down to 0.07-0.08 J/cm^2. In case of 100 pulses the variations are bigger, without showing any clear tendency. This is possibly caused by bigger measuring error for more shallow craters, if compare to 250 pulses. The Top Hat beam profile shows an almost two times higher threshold fluence compared to the values obtained for Gaussian profile. This may be the reason for measured lower specific removal rate for the Top Hat profile.

In figure 5, the energy penetration depth for the Gaussian and the Top Hat beam profile is shown. For a Gaussian beam a drop for spot sizes at 60 µm can be observed. A strong incubation effect is observed just for Gaussian beam.

3.2. 350 fs pulse duration

Figure 6 shows the measured specific removal rates for different spot sizes for Gaussian beam shape with 350 fs pulse duration for constant number of machined layers and overlap. Similar as in case of the 10 ps study, a 20% decrease of the specific removal rate is observed when the spot size is increasing from approximately 15 µm to 60 µm. As expected, shorter pulse durations cause an increase of the specific removal rate by a factor of 2.5 compared to 10 ps pulse duration.

The threshold fluence and energy penetration depth deduced following (6) is presented in table 1 and show a decrease in both measures with increasing laser spot size. The same range of values of threshold fluence was obtained for 10 ps pulse duration (between 0.05 and 0.1 J/cm^2). In contrast, the energy penetration depth reached values higher than that for 10ps for Gaussian and Top Hat profile. This confirms the correlation between specific removal rate and energy penetration depth [17].

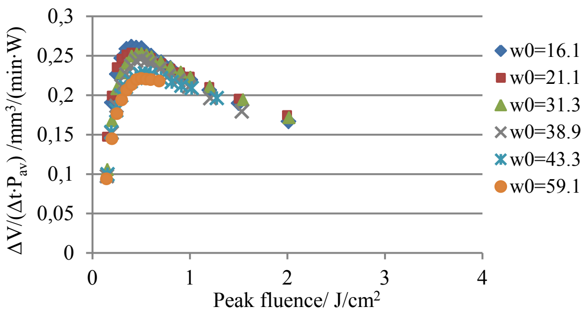

Fig. 6. Influence of the Gaussian beam spot size on the specific removal rate as function of peak fluence for 350 fs pulse duration by machining squares.

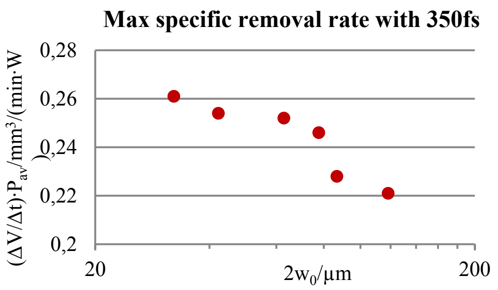

Fig. 7. Influence of the Gaussian spot size on the maximum specific removal rate for 350 fs pulse duration by machining squares.

Table 1. Threshold fluence and energy penetration depth obtained for different spot sizes for 350 fs pulse duration.

Beam radius, w_0 (µm)	Threshold fluence (J/cm^2)	Energy penetration depth (nm)
16.1	0.060	9.4
21.1	0.059	9.3
31.3	0.064	9.9
38.9	0.070	10.4
43.3	0.073	10.2
59.1	0.076	10.4

4. Conclusions

The influence of the laser beam spot size and shape onto specific removal rate was investigated for 10 ps and 350 fs pulse duration. For a Gaussian beam, both, ps and fs pulse duration, show a 20%, almost linear, decrease of maximum specific removal rate with increasing spot size. However, this behavior is only clearly visible for radii bigger than 20µm.

Unexpectedly, the Top Hat beam profile shows just a slight decrease of 8%. As in case of Gaussian beam shape, there is a certain point (spot size) when the specific removal rate started to decrease. It is possible that for Top Hat profile, spot size effect is more pronounces for spots sizes much bigger than 63µm.

References

[1] Chichkov B.N, Momma C, Nolte F, von Alvensleben F, Tünnermann A. Femptosecond, picosecond and nanosecond laser ablation of solids. Appl Phys 1996;A6:109.

[2] Dausinger F, Hügel H, Konov V. Micro-machining with ultrashort laser pulses: From basic understanding to technical applications. Proc. SPIE 2003;5147:106-115.

[3] Neuenschwander B, Jaeggi B, Schmid M, Henning G, Surface Structuring with Ultra-short Laser Pulses: Basics, Limitations and Needs for High Throughput. Physics Procedia 2014;56:1047-1058.

[4] Raciukaitis G, Brikas M, Grecys P, Voisiat B, Gedvilas M. Use of high repetition rate and high power lasers in microfabrication: How to keep the efficiency high?. JLMN-Journal of Laser Micro/Nanoengineering 2009;4(3).

[5] Neuenschwander B, Bucher GF, Henning G, Nussbaum C, et al. Processing of dielectric materials and metals with ps laser pulses. ICALEO 2010; Paper M101.

[6] Neuenschwander B, Jaeggi B, Schmid M, From fs to Sub-ns: Dependence of the material removal rate and the surface quality on the pulse duration for metals, semiconductors and oxides. ICALEO 2012;M1004.

[7] Hänel N, Stolze M, Hermann T, Lhuillier J. Fundamental investigations of ps-laser burst-mode on common metals for an enhanced ablation process. Proc. SPIE 2015;9351.

[8] Kramer T, Neuenschwander B, Jaeggi B, Remund S, Hunziker U, Zürcher J. Influence of pulse bursts on the specific removal rate for ultra-fast pulsed laser micromachining of copper. Physics Proc. 2016;86:123-134.

[9] Jaeggi B, Neuenschwander B, Hunziker U, Zürcher J, Meier T, Zimmermann M, Selbmann KH, Hennig G, Ultra-high-precision surface structuring by synchronizing a galvo scanner with an ultra-short-pulsed laser system in MOPA arrangement. Proc. SPIE (2012);8243.

[10] Eyett M, Bäuerle D. Influence of the beam spot size on ablation rates in pulsed-laser processing. Appl. Phys. Lett. 1987;51:2054.

[11] Martin S, Hertwig A, Lenzner M, Krüger J, Kautek W. Spot-size dependence of the ablation threshold in dielectrics for femtosecond laser pulses. Appl. Phys. 2003;A77:883-884.

[12] Wolff-Rottke B, Ihlemann J, Schmidt H, Scholl A. Influence of the laser spot diameter on photo-ablation rates. Appl. Phys.1995. A Mater. Sci. Process;60(1):13-17.

[13] Zweig AD. A thermo-mechanical model for laser ablation. Appl. Phys. 1991;70(3):1684-1691.

[14] Lauer B, Jaeggi B, Zhang Y, Neuenschwander B. Measurement of the maximum specific removal rate: unexpected influence of experimental method and the spot size. ICALEO 2015;M701.

[15] Shaheen ME, Gagnon JE, Fryer BJ. Excimer laser ablation of aluminum: influence of spot size on ablation rate. Laser Phys. 2016;26:116102.

[16] Brandi F, Burdet R, Caryino R, Diaspro A. Very large spot size effect in nanosecond laser drilling efficiency of silicon. Optics Express 2010;22(18):23488-23494.

[17] Neuenschwander B, Jaeggi B, Schmid M, Rouffiange V, Martin P. Optimalization of the volume ablation rate for metals at different laser pulse durations from ps to fs. SPIE Proceedings (2012);824307.

[18] Neuenschwander B, Bucher GF, Nussbaum C, Joss B, Muralt M, Hunziker U, Schuetz P. Processing of metals and dielectric materials with ps-laserpulses: results, strategies, limitation and needs. SPIE Proceedings (2010);7584.
[19] Ancona A, Döring S, Jauregui C, Röser F, Limpert J, Nolte S, Tünnermann A. Femptosecond and picosecond laser drilling of metals at high repetition rates and average powers. Optics Letters 2009;34(21):3304-3306.
[20] Jaeggi B, Neuenschwander B, Remund S, Kramer T. Influence of pulse duration and the experimental approach onto the specific removal rate for ultra-short pulses. SPIE Proceedings (2017);100910J.